Journal of Proteins and Proteomics (2021) 12:213–226
https://doi.org/10.1007/s42485-021-00069-8

ORIGINAL ARTICLE

Identification of effective and specific serotonin$_{1B}$ receptor ligands by structure-based virtual screening and molecular dynamics

Bhawani Prasad Bag[1] · **Sameer Saurava Prusty**[2] · **Amiya Kumar Patel**[1]

Received: 22 April 2021 / Revised: 26 June 2021 / Accepted: 7 July 2021 / Published online: 15 July 2021

Abstract

The serotonergic systems are the most important therapeutic targets for neurological disorders. Many serotonergic drugs have been used to treat neurological disorders, which are well known for their adverse side effects because of the off-target interactions. Development of selective ligands for a specific target is the suitable approach to minimize the off-target interactions and side effects. To identify selective ligands for serotonin 1B receptor (5-HT$_{1B}$R), the structural analogs of inverse agonist methiothepin (MT) and natural products were screened against 5-HT$_{1B}$R and other 5-HTR subtypes (5-HT$_{2A}$R, 5-HT$_{2B}$R, and 5-HT$_{2C}$R). In the present study, five compounds were selected out of 9963 screened compounds having higher binding affinity with 5-HT$_{1B}$R over other 5-HTRs. Amongst them, ZINC31166967 and ZINC31162553 exhibited relatively higher binding affinity towards 5-HT$_{1B}$R with the binding energy of − 10.1 and − 9.1 kcal/mol, respectively. The pharmacokinetic assessments considered them safe and non-toxic. Molecular dynamics (MD) simulation revealed the stability of these compounds within the active site of the receptor. The overall analysis suggested that ZINC31166967 and ZINC31162553 may be considered as the selective ligands for 5-HT$_{1B}$R. However, detailed experimental investigations will be required to substantiate the findings.

Keywords Serotonin receptor · 5-HT$_{1B}$ receptor · Natural products · Drug-like molecules · Virtual screening · MD simulation

Introduction

The G protein-coupled receptors (GPCRs) are the largest family of cell surface receptor proteins in mammalian genome (Fredriksson et al. 2003) and are targeted by approximately 34% of the Food and Drug Administration (FDA) approved drugs (Hauser et al. 2018). Amongst all, serotonin (5-hydroxytryptamine or 5-HT) receptors have been considered as suitable therapeutic targets because of their association with diverse signaling pathways related to several physiological and behavioral functions (Berger et al. 2009). The serotonin 1B receptors (5-HT$_{1B}$Rs) are involved in locomotion, sleep, thermoregulation, mood disorder, pain modulation, impulsivity, aggression, memory and learning (Cao et al. 2013; Tiger et al. 2018; Lanfumey and Hamon 2004; Sari 2004). Upon agonist binding, 5-HT$_{1B}$R is negatively coupled with $G_{i/o}$ family of proteins and inhibits adenylyl cyclase (AC) that leads to decrease in the formation of cyclic adenosine monophosphate (cAMP) and consequently, results in the reduction of 5-HT release. In contrast, the selective antagonist binding increases 5-HT release in synaptic cleft which is the basis of designing of the potential antidepressant drugs (Yin et al. 2018). The 5-HT$_{1B}$R agonists are being used clinically as antimigraine drugs and potential therapeutics for anti-aggressive, bipolar disorder, gastric motor effects, and autism. On the other hand, antagonists are considered effective antidepressant agents (Slassi 2002).

Many serotonergic drugs show adverse side effects because of the off-target interactions. Thus, attention to the development of selective agonists and antagonists for 5-HT$_{1B}$R has been increased enormously. It is challenging to design subtype-specific serotonergic ligands due to

✉ Bhawani Prasad Bag
bpbag@suniv.ac.in; bhawaniprasad@gmail.com

✉ Amiya Kumar Patel
amiya.gene@gmail.com

[1] Department of Biotechnology and Bioinformatics, Sambalpur University, Jyoti Vihar, Sambalpur 768019, India

[2] Department of Zoology, Government Autonomous College, Rourkela 769004, India

high sequence similarity/identity and structural conservation among the 5-HT receptors. Many crystal structures of 5-HT_{1B}R, 5-HT_{2A}R, 5-HT_{2B}R, and 5-HT_{2C}R complexed with agonists and antagonists have been reported (Yin et al. 2018; Wang et al. 2013; Kimura et al. 2019; Kim et al. 2020; Wacker et al. 2013, 2017; McCorvy et al. 2018; Peng et al. 2018). The comparative structural analysis of 5-HT_{1B}R and 5-HT_{2B}R supplements valuable information for subtype selectivity (Wacker et al. 2013; McCorvy and Roth 2015). The 5-HT_{1B}R in complex with inverse agonist methiothepin (MT) provides the structural understanding of ligand-induced repression activity of the receptor (Yin et al. 2018). Evaluation of chemical activities of different compounds against specific receptors using in silico techniques is widely used and accepted approach in pharmaceutical industries. The objective of the present study is to identify the specific and effective ligands for 5-HT_{1B}R with minimal side effects based on the inverse agonist structure. To find selective 5-HT_{1B}R ligands, several compounds were screened based on properties similar to inverse agonist MT and natural compounds collected from the ZINC database against the orthosteric binding sites of 5-HT_{1B}R and other 5-HTRs. Besides, the results were compared with the binding affinities of known 5-HT_{1B}R antagonists.

Computational details

Preparation of receptor proteins and ligands

The crystal structures of 5-HT_{1B}R (PDB ID: 5V54) (Yin et al. 2018), 5-HT_{2A}R (PDB ID: 6A93) (Kimura et al. 2019), 5-HT_{2B}R (PDB ID: 4IB4) (Wacker et al. 2013), and 5-HT_{2C}R (PDB ID: 6BQG) (Peng et al. 2018) were retrieved from Protein Data Bank (http://www.rcsb.org/) (Berman et al. 2000). All the nonprotein atoms and fusion protein insertion were removed from all the receptor proteins and processed before molecular docking. The missing residues in extracellular loop 2 (ECL2) (AEEEV) and ECL3 (KDAC) of 5-HT_{1B}R were modeled using a loop modeling database by Chimera 1.11 and Modeller (Pettersen et al. 2004; Webb and Sali 2016). The polar hydrogen and Kollman charges were assigned to the receptor protein using AutoDock Tools.

Two sets of ligands were used to identify the effective and specific potential candidates for 5-HT_{1B}R. The first dataset (DS1) comprises drug-like molecules having properties similar to inverse agonist MT. The drug-like molecules with molecular weight (MW) ranging from 340 to 390 g/mol, octanol/water partition coefficient (logP): 1.5–5, net charge: − 1–1, rotatable bond: 0–8, hydrogen donors: 0–6, hydrogen acceptors: 0–8, polar surface area: 30–70 ($Å^2$), polar desolvation: − 20–1 kcal/mol, apolar desolvation: 5–30 kcal/mol were acquired using properties search option of ZINC12 database (https://zinc12.docking.org/) (Irwin et al. 2012). The second dataset (DS2) consists of natural products from the different sub-databases available in ZINC database (Sterling and Irwin 2015). The downloaded molecules were minimized with universal force field (UFF), a non-reactive classical force field that contains parameters for every atom of the periodic table (Rappé et al. 1992; Jaillet et al. 2017) using PyRx tool (Dallakyan and Olson 2015). All the minimized ligands were converted to.pdbqt format for virtual screening.

Virtual screening

A total of 9963 compounds were virtually screened using AutoDock Vina (Trott and Olson 2010). The screened compounds comprised drug-like molecules similar to MT (4970 candidates) and natural compounds (4993 candidates) from the ZINC database. Since MT binds deep into the hydrophobic orthosteric binding pocket of 5-HT_{1B}R, all the selected compounds were docked to the orthosteric binding pocket. To identify the selective molecules for 5-HT_{1B}R, they were further docked to other 5-HTR subtypes such as 5-HT_{2A}R, 5-HT_{2B}R, and 5-HT_{2C}R. A grid box of size 18 Å × 20 Å × 22 Å (*x*, *y*, *z* dimension) centered at − 7.494, − 17.962, and 23.548 Å was used for 5-HT_{1B}R. Similarly, the grid box size of 24 Å × 22 Å × 20 Å centered at 15.775, 0.734, 59.499 Å for 5-HT_{2A}R, 18 Å × 18 Å × 20 Å centered at 23.59, 16.17, 7.031 Å for 5-HT_{2B}R, 24 Å × 22 Å × 24 Å centered at 22.238, 33.962, 55.13 Å for 5-HT_{2C}R were set. The grid spacing was set to 1 Å. The compounds with higher binding affinities than MT against 5-HT_{1B}R and lower affinities for other 5-HTRs were identified and analyzed for predictive pharmacokinetics and toxicological activities. Molecular interactions were visualized and the plots were generated using Chimera 1.11 and LigPlot + (Pettersen et al. 2004; Laskowski and Swindells 2011).

Drug-likeness and ADMET analysis

Lipinski's rule of five (RO5) (Lipinski 2004) and fragment-based method (Sander et al. 2015) was adopted to determine the drug-like properties of all the selected compounds. Properties like absorption, distribution, metabolism, excretion, and toxicity (ADMET) were analyzed using admetSAR 2.0 (Yang et al. 2019) and DataWarrior 5.2.1 (https://openmolecules.org/) (Sander et al. 2015). The admetSAR 2.0 server has over 200,000 experimental data for 96,000 unique compounds and more than 40 computational models to predict ADMET properties (Yang et al. 2019). The server evaluates drug-likeness of a compound from different ADMET properties such as human intestinal absorption (HIA), Caco-2 permeability (Caco-2), blood–brain barrier (BBB), organic cation transporter protein 2 inhibitor (OCT2i), P-glycoprotein inhibitor and substrate (P-gps and P-gpi), cytochromes

P450 (CYPs) substrates and inhibitors, Ames mutagenesis, carcinogenicity, acute oral toxicity (AOT), etc. The predicted properties were described by words or values associated with a probability that denotes the accuracy of the features. DataWarrior is an interactive data visualization and analysis program, which predicts molecular properties such as MW, logP, water solubility (logS), and topological polar surface area (TPSA) from chemical structures. It also predicts major toxicological features like mutagenicity, tumorigenicity, irritating effects, and reproductive effects. DataWarrior computes fragment-based drug-likeness score using a data set of 5300 distinct sub-structure fragments generated from drugs and commercially available chemical blocks. The drug-likeness score (d) was calculated by the following equation:

$$d = \frac{\sum v_i}{\sqrt{n}},$$

where 'v_i' is the score value of sub-structure fragment under observation and 'n' is the fragment count. A positive score indicates that the compound of interest has sub-structure fragments often present in commercially available drugs (Sander et al. 2015). In this study, the pharmacokinetic properties such as HIA, Caco-2, BBB, CYP2D6 inhibition, Ames mutagenesis, AOT, carcinogenicity, and biodegradation were analyzed.

Molecular dynamics (MD) simulation

The binding stability of the efficiently docked complexes was analyzed through MD simulation for 100 ns time scale using GROMACS 2019 (Abraham et al. 2015). The topology of 5-HT_{1B}R was generated using GROMOS96 53a6 force field (Oostenbrink et al. 2004; Shukla et al. 2019, 2018). GROMOS96 53a6 force field is widely used to calculate solvation free energy of amino acid side chains and in protein simulations (Oostenbrink et al. 2005). Molecular topologies and coordinates of the selected compounds were generated by PRODRG server (Schüttelkopf and Aalten 2004). Each system was solvated with simple point charge (SPC) water model in a cubic box of 1.4 nm dimensions and neutralized with appropriate ions. Energy minimization was performed using the steepest descent algorithm to remove steric clashes. The accuracy of short-range interactions during the simulation suffers because of the long-range interactions. GROMACS uses several methods such as the Ewald summation method (Hummer 1995), Particle Mesh Ewald (PME) method (Essmann et al. 1995), and Particle–Particle*** Particle–Mesh (PPPM) method (Deserno and Holm 1998) to calculate long-range interactions during the computation. PME has been widely used method because of its low computational complexity (Zhang et al. 2019), which was used in the study to handle the long-range electrostatic interactions with a cut-off of 1.2 nm. The hydrogen bond lengths were constrained using LINear Constraint Solver (LINCS) algorithm (Hess et al. 1997). The LINCS algorithm resets bonds to their correct lengths in two steps following an unconstrained update. First, the new bonds' projections on the old bonds are set to zero. Then, a correction for bond lengthening due to rotation is applied. The LINCS algorithm is more stable, 3–4 times faster than the SHAKE algorithm, and suitable for large molecules (Hess et al. 1997). The equilibration for each system was carried out in the constant number of particles, volume, and temperature (NVT) and the constant number of particles, pressure, and temperature (NPT) conditions for 10 ns. The temperature and pressure coupling parameters were V-rescale and Parrinello–Rahman method, respectively (Bussi et al. 2007; Parrinello and Rahman 1981). The V-rescale algorithm is a modified Berendsen thermostat using velocity rescaling with an additional stochastic term that ensures proper canonical ensemble (Bussi et al. 2007). The MD cell in Parrinello–Rahman method is allowed to change its shape and volume to comply with the structural phase transition using a Lagrangian formulation (Parrinello and Rahman 1981). Finally, all the equilibrated systems were subjected to 100 ns MD simulation. All processes were carried out in triplicates to minimize error and ensure the stability of the systems. The average values were used for the analysis. The root mean square deviation (RMSD), root mean square fluctuation (RMSF), the radius of gyration (Rg), solvent accessible surface area (SASA), and total numbers of hydrogen bonds were calculated from the trajectory files.

Results and discussion

A total of 9963 compounds (analogs of MT and natural compounds) were virtually screened against the orthosteric binding pocket of 5-HT_{1B}R and subsequently against 5-HT_{2A}R, 5-HT_{2B}R and 5-HT_{2C}R to identify the receptor-specific ligands. All the compounds were downloaded from ZINC database, a free public database consisting of ready-to-dock commercially available compounds (Irwin et al. 2012; Sterling and Irwin 2015). The key residues of the binding pocket of 5-HTRs are shown in Table 1. The Ballesteros–Weinstein numbering is used to represent the binding site residues (Ballesteros and Weinstein 1995).

Virtual screening and docking studies

Virtual screening was performed using AutoDock Vina and the key residues of binding pockets were kept within the screening space. For each compound, twenty distinct poses were generated and the best pose was selected based on

Table 1 Important residues involved in the binding pocket of 5-HT_{1B}R, 5-HT_{2A}R, 5-HT_{2B}R and 5-HT_{2C}R

Receptor	PDB ID	Ligand Binding Pocket* Orthosteric and extended pocket residues
5-HT_{1B}	5V54	W125$^{3.28}$, L126$^{3.29}$, D129$^{3.32}$, I130$^{3.33}$, C133$^{3.36}$, T134$^{3.37}$, V200^{ECL2}, V201^{ECL2}, T203^{ECL2}, Y208$^{5.38}$, T209$^{5.39}$, S212$^{5.42}$, A216$^{5.46}$, W327$^{6.48}$, F330$^{6.51}$, F331$^{6.52}$, S334$^{6.55}$, M337$^{6.58}$, P338$^{6.59}$, F351$^{7.35}$, D352$^{7.39}$, T355$^{7.39}$, Y359$^{7.43}$
5-HT_{2A}	6A93	S131$^{2.61}$, W151$^{3.28}$, D155$^{3.32}$, V156$^{3.33}$, S159$^{3.36}$, T160$^{3.37}$, I163$^{3.37}$, L228^{ECL2}, L229^{ECL2}, V235$^{5.39}$, G238$^{5.42}$, S242$^{5.46}$, F243$^{5.47}$, F332$^{6.44}$, W336$^{6.48}$, F339$^{6.51}$, F340$^{6.52}$, L362$^{7.35}$, N363$^{7.36}$, V366$^{7.39}$, Y370$^{7.43}$
5-HT_{2B}	4IB4	W131$^{3.28}$, L132$^{3.29}$, D135$^{3.32}$, V136$^{3.33}$, S139$^{3.36}$, T140$^{3.37}$, V208^{ECL2}, L209^{ECL2}, K211^{ECL2}, F217$^{5.38}$, M218$^{5.39}$, G221$^{5.42}$, A225$^{5.46}$, W337$^{6.48}$, F340$^{6.51}$, F341$^{6.52}$, N344$^{6.55}$, L347$^{6.58}$, V348$^{6.59}$, L362$^{7.35}$, E363$^{7.36}$, V366$^{7.39}$, Y3707$^{.43}$
5-HT_{2C}	6BQG	W130$^{3.28}$, D134$^{3.32}$, V135$^{3.33}$, S138$^{3.36}$, T139$^{3.37}$, V208^{ECL2}, L209^{ECL2}, F214$^{5.38}$, V215$^{5.39}$, G218$^{5.42}$, A222$^{5.46}$, W324$^{6.48}$, F327$^{6.51}$, F328$^{6.52}$, N331$^{6.55}$, S334$^{6.58}$, V335$^{6.59}$, L350$^{7.35}$, N351$^{7.36}$, V354$^{7.39}$, Y358$^{7.43}$

*Data source (Yin et al. 2018; Kimura et al. 2019; Wacker et al. 2013; Peng et al. 2018). Superscripts refer to the Ballesteros-Weinstein numbering scheme (Ballesteros and Weinstein 1995)

binding energy and hydrogen bond interaction. The results of virtual screening were filtered in multiple steps to identify the selective ligands for 5-HT_{1B}R. The overall methodology is demonstrated in Fig. 1.

All the 9963 compounds, MT, and zotepine were screened against 5-HT_{1B}R and the binding energies were recorded. The binding energy of MT was found to be − 8.8 kcal/mol. A total of 190 drug-like and 1543 natural compounds with higher affinities than MT were selected. The selected compounds were scrutinized for drug-likeness score using DataWarrior. A total of 392 compounds were found to have a positive drug-likeness score. Out of 392 compounds, 46 drug-like and 209 natural compounds were recognized as cleaned molecules based on the toxicity risk assessments. To identify the selectivity of 5-HT_{1B}R over other 5-HTRs, these compounds were further docked with 5-HT_{2A}R, 5-HT_{2B}R

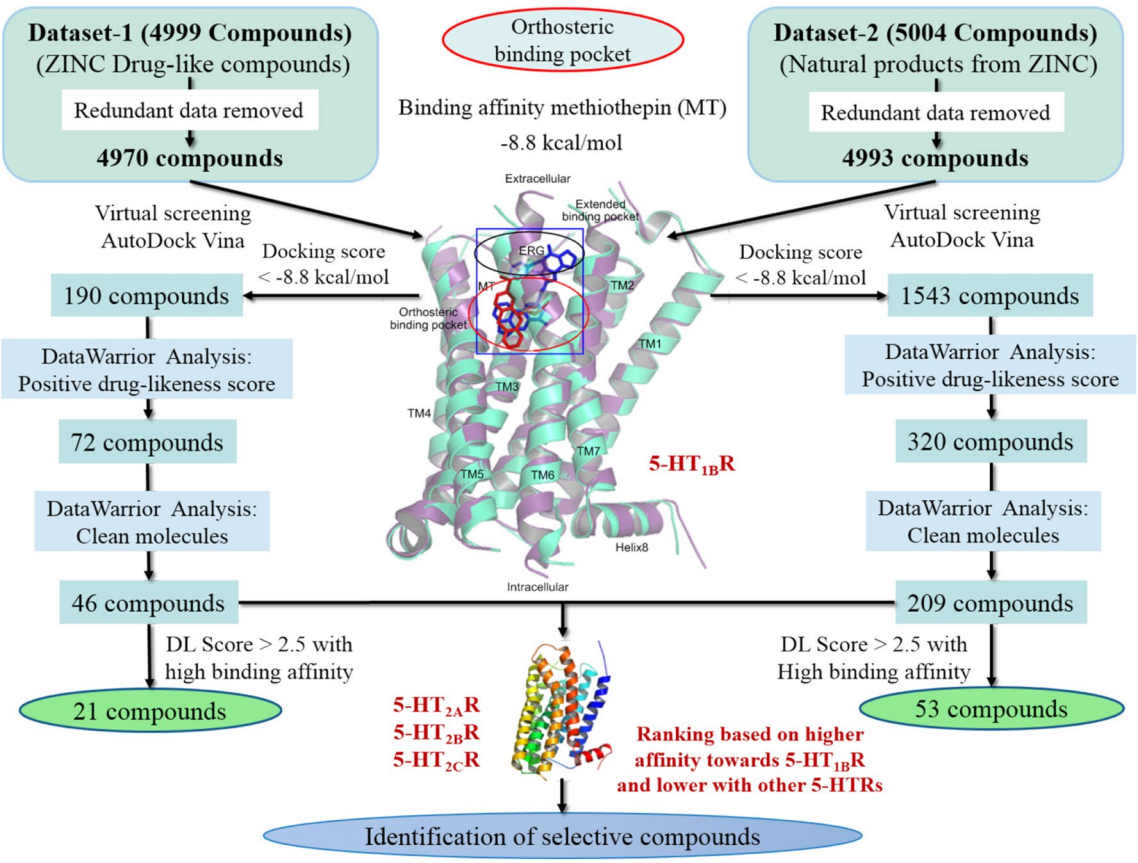

Fig. 1 Schematic representation of overall workflow to identify selective ligands for 5-HT_{1B}R

and 5-HT_{2C}R. Compounds having higher binding affinity with other 5-HTRs were discarded (Supplementary data Table S1). Compounds with higher binding affinity with 5-HT_{1B}R and drug-likeness score greater than 2.5 were selected. Finally, five natural compounds (ZINC31166967, ZINC31166959, ZINC31166963, ZINC13367860, and ZINC31162553) and two drug-like compounds analog to MT (ZINC54661486 and ZINC78877086) were identified and analyzed. The binding energies of the shortlisted compounds against 5-HT_{1B}R varied between − 10.1 and − 9.1 kcal/mol. The comparative binding energy chart of the top-ranked compounds towards 5-HT_{1B}R and other 5-HTRs is shown in Fig. 2. Site-specific docking results of the selected compounds, MT, and zotepine with 5-HT_{1B}R are listed in Table 2.

5-HT_{1B}–MT and 5-HT_{1B}–zotepine complexes

The binding energy of MT and zotepine were estimated to be − 8.8 and − 8.4 kcal/mol, respectively. It is evident from the study that MT formed one hydrogen bond with D129 (3.28 Å), whereas zotepine formed two hydrogen bonds with S212 (3.33 Å) and S334 (2.97 Å). Besides, the complexes were further stabilized through hydrophobic interactions with various active site residues.

5-HT_{1B}–natural compound complexes

The study revealed that ZINC31166967 displayed the lowest binding energy of − 10.1 kcal/mol among all the selected compounds. ZINC31166967 formed four hydrogen bonds with S212 (2.97 Å), T213 (3.2 Å), S334 (2.81 Å), and Y359 (2.67 Å) of 5-HT_{1B}R. Additionally, the residues W125, L126, I130, C199, V200, V201, F330, F331, M337, F351, D352, and T355 provided stability to 5-HT_{1B}–ZINC31166967 complex through hydrophobic interactions (Fig. 3a). Both ZINC31166959 and ZINC31166963 formed one hydrogen bond with residue Y359 with the binding energy of − 10 and − 9.2 kcal/mol, respectively (Fig. 3b, c). The hydrophobic interactions between the ligand and different residues of orthosteric/extended binding site provided additional stability to the complex. Since ZINC31166967, ZINC31166959, and ZINC31166963 are conformational isomers,

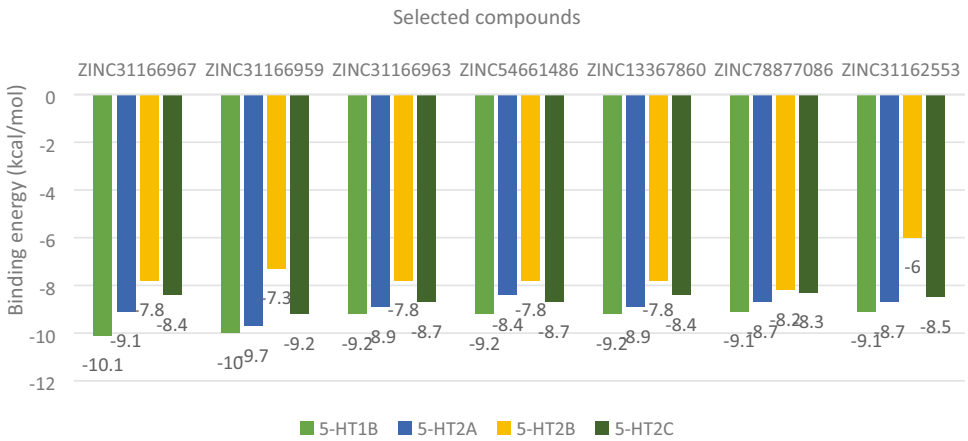

Fig. 2 Cluster column representing binding energy (kcal/mol) of the selected compounds against 5-HT_{1B}R and other 5-HTRs (5-HT_{2A}R, 5-HT_{2B}R, and 5-HT_{2C}R)

Table 2 Results of docking analysis of the selected compounds along with reference inhibitor and antagonist with 5-HT_{1B}R

Compounds	Binding energy (kcal/mol)	Residue(s) involved in hydrogen bonding	Distance (Å)
Drug-like and natural compounds			
ZINC31166967	− 10.1	S212, T213, S334, Y359	2.97, 3.20, 2.81, 2.67
ZINC31166959	− 10	Y359	3.05
ZINC31166963	− 9.2	Y359	3.09
ZINC54661486	− 9.2	S212	2.85
ZINC13367860	− 9.2	I130, T134	2.91, 3.08
ZINC78877086	− 9.1	S106, Y359	3.35, 2.60
ZINC31162553	− 9.1	D129, S212, S334, M337	2.91, 2.97, 2.87, 2.93
Reference and known 5-HT_{1B}R antagonist			
Methiothepin	− 8.8	D129	3.28
Zotepine	− 8.4	S212, S334	3.33, 2.97

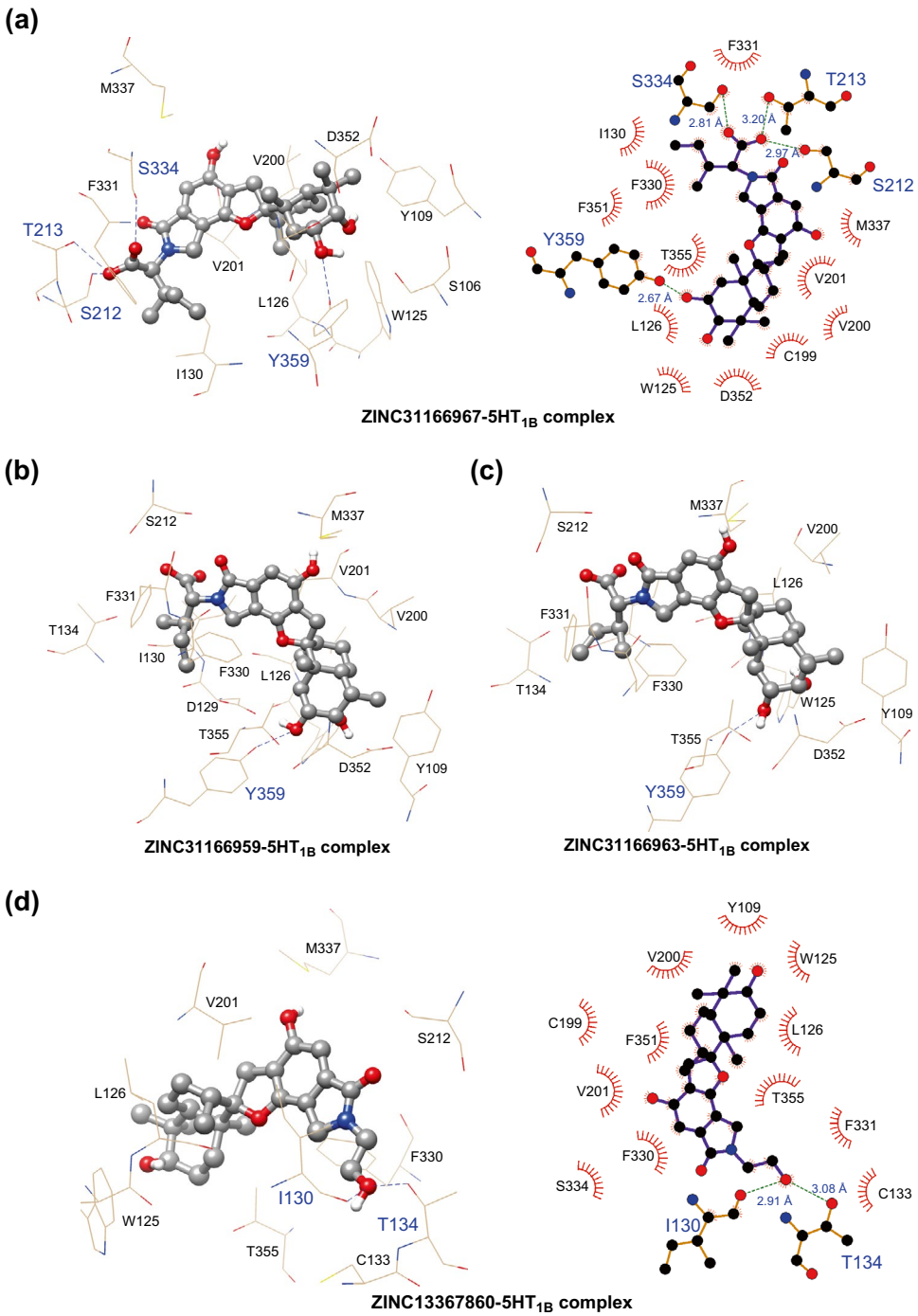

Fig. 3 The poses and 5-HT_{1B}–ligand interactions for five selected natural compounds **a** ZINC31166967, **b** ZINC31166959, **c** ZINC31166963, **d** ZINC13367860, and **e** ZINC31162553. Selected compounds are shown in ball and stick form and binding pocket residues are shown in wires. Hydrogen bonds are indicated by blue dashed line, while hydrophobic contacts are shown in red arc with spokes radiating towards the ligand

ZINC31166967 was only considered for further analysis because of lowest binding energy and highest number of hydrogen bonds with the receptor. The interaction between 5-HT_{1B}–ZINC13367860 docked complex showed two hydrogen bonds with I130 (2.91 Å) and T134 (3.08 Å) with binding energy of − 9.2 kcal/mol. In addition, the residues Y109, W125, L126, C133, C199, V200, V201, F330, F331, S334, F351, and T355 were involved in hydrophobic interactions stabilizing the complex (Fig. 3d). The binding energy of ZINC31162553 towards 5-HT_{1B}R was − 9.1 kcal/mol. ZINC31162553 interacted with 5-HT_{1B}R via four hydrogen bonds (D129, S212, S334, and M337 with the distance of 2.91 Å, 2.97 Å, 2.87 Å, and 2.93 Å, respectively). The stability of the complex was further supported by hydrophobic interactions with the residues Y109, W125, I130, C133, T134, I180, V200, V201, W327, F330, F331, F351, and T355 (Fig. 3e).

Fig. 3 (continued)

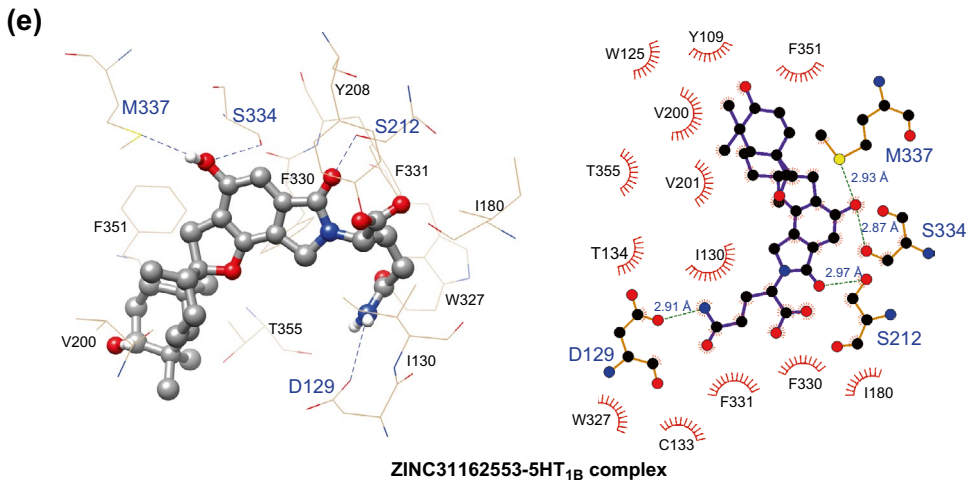

5-HT$_{1B}$–drug-like compound complexes

The study suggested that ZINC54661486 and ZINC78877086 showed binding energy of − 9.2 and − 9.1 kcal/mol, respectively. ZINC54661486 formed only one hydrogen bond with S212 (2.85 Å) and the hydrophobic interactions with residues D129, I130, C133, T134, V201, T209, T213, A216, W327, F330, F331, S334, and T355 of 5-HT$_{1B}$R (Fig. 4a). The 5-HT$_{1B}$–ZINC78877086 complex was stabilized with the formation of two hydrogen bonds by residues S106 (3.35 Å) and Y359 (2.6 Å). Besides, residues A216, F331, S212, C133, D129, T355, D352, W125, Y109, F330, W327, V201, and I130 were found to be associated with hydrophobic interactions (Fig. 4b).

Further, ZINC31166967, ZINC54661486, ZINC13367860, ZINC78877086, and ZINC31162553 were selected for the pharmacokinetic assessments. The chemical structures of the selected compounds are depicted in Fig. 5.

Drug-likeness and ADMET studies

The physicochemical and pharmacokinetic properties play crucial role in the development of new drugs. All the compounds with good binding affinity with 5-HT$_{1B}$R were evaluated for drug-likeness and ADMET to eliminate undesirable features. The physicochemical properties such as MW, TPSA, logP, hydrogen bond acceptors (HA), hydrogen bond donors (HD), and drug-likeness score were assessed and listed in Table 3. The molecular weight of ZINC31166967 and ZINC31162553 was found to be relatively higher (515.65 and 514.62 g/mol, respectively) compared to the suggested value (≤ 500 g/mol). However, this value is acceptable for natural compounds. TPSA of all the selected compounds was found in the range of 59.23 to 150.39 Å^2. TPSA describes the sum of PSA values of polar fragment of a compound and is an important parameter for the prediction of molecular permeability (Fernandes and Gattass 2009). The recommended TPSA cut-off is 140–150 Å^2 (Lipinski 2008). The percentage absorption (%Abs) was calculated using the following equation (Zhao et al. 2002; Bhowmik et al. 2021):

$$\%\text{Abs} = 109(0.345 \times \text{TPSA}).$$

The %Abs of all the selected compounds were found to be relatively lower compared to MT and zotepine. The study suggested that ZINC31166967 (65%) and ZINC31162553 (57.1%) showed lower %Abs, because of their higher MW, HA and HD moieties. However, all the compounds showed %Abs greater than 50%, which suggested good bioavailability exhibited by the compounds. The LogP value determines the solubility and permeability of a molecule. The LogP values of these compounds were found to be less than 5 (range 2.06–3.86), which suggested their good permeation and distribution in biological system. The physicochemical evaluation revealed that all the selected compounds showed suitable drug-like properties. The pharmacokinetic properties were examined and listed in Table 4 and Table S2 (Supplementary data). The oral bioavailability of a drug is preliminary controlled by intestinal absorption. The admetSAR predicted values were labeled as HIA + (absorbable) or HIA- (nonabsorbable). All the compounds displayed good intestinal absorption with probability ranging from 0.95 to 0.99. The Caco-2 cell line model is also widely used for the prediction of human intestinal absorption (Hou et al. 2004; Pham The et al. 2011). All the compounds showed negative Caco-2 permeability except ZINC54661486 and ZINC13367860. The BBB permeability is a significant aspect to be considered in drug discovery. Neuroactive drugs must cross the BBB (BBB +), whereas peripherally acting drugs must not cross the BBB (BBB-) to avoid unwanted central

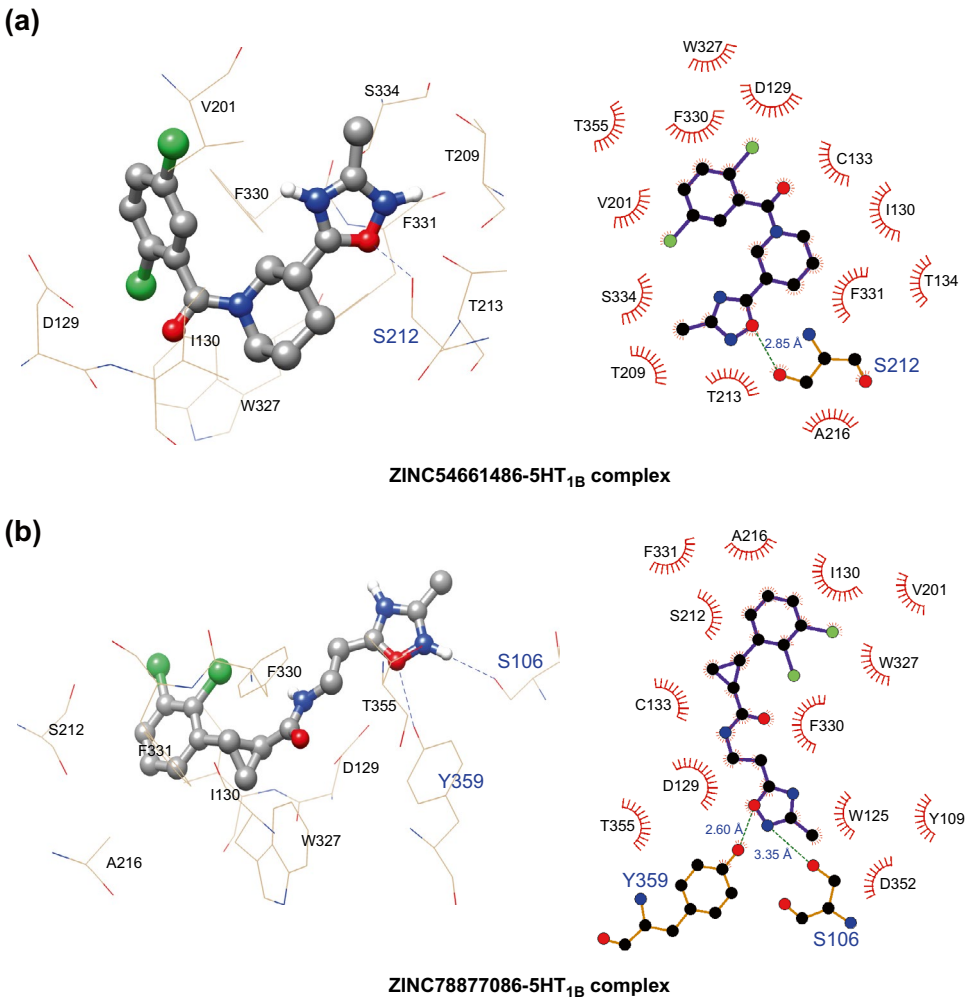

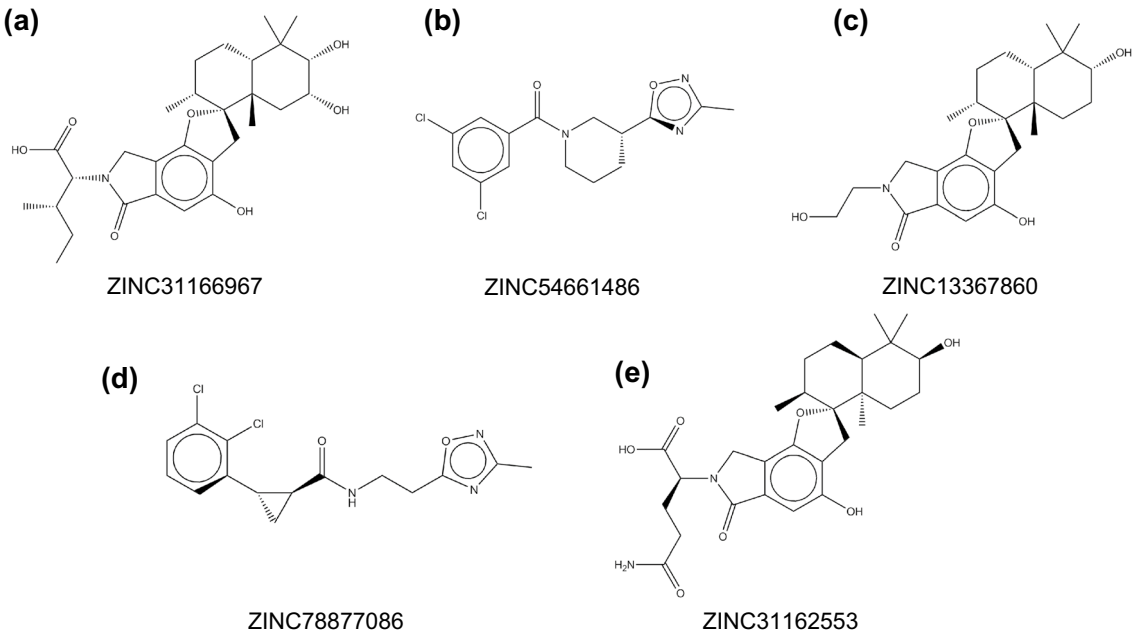

Fig. 4 The poses and 5-HT_{1B}–ligand interactions for two selected drug-like compounds **a** ZINC54661486 and **b** ZINC78877086. Selected compounds are shown in ball and stick form and binding pocket residues are shown in wires. Hydrogen bonds are indicated by blue dashed line, while hydrophobic contacts are shown in red arc with spokes radiating towards the ligand

Fig. 5 Chemical structure of the selected compounds

Table 3 Physicochemical properties and drug-likeness of the selected compounds

Dataset	Compounds	MW	TPSA	LogP	HA	HD	NLV	%Abs	DL
DS2	ZINC31166967	515.65	127.53	3.10	8	4	1	65.00	3.342
DS1	ZINC54661486	340.21	59.23	3.86	5	0	0	88.56	7.329
DS2	ZINC13367860	429.46	90.23	2.81	6	3	0	77.87	2.686
DS1	ZINC78877086	340.21	68.02	3.18	5	1	0	85.53	4.325
DS2	ZINC31162553	514.62	150.39	2.06	9	4	1	57.11	3.849
Methiothepin (MT)		356.56	57.08	4.42	2	0	0	89.30	7.811
Zotepine		331.86	37.77	4.67	2	0	0	95.96	4.874

DS1 dataset-1, *DS2* dataset-2, *MW* molecular weight (g/mol) (130–725), *TPSA* topological polar surface area (Å^2) (< 150 Å^2), *logP* predicted octanol/water partition coefficient (≤ 5), *HA* hydrogen bond acceptor (≤ 10), *HD* hydrogen bond donor (≤ 5), *NLV* number of Lipinski rule violation (≤ 1), *%Abs* absorption percentage (> 50%), *DL* drug-likeness score

Table 4 Pharmacokinetics and toxicity analysis of the selected compounds

Dataset	Compounds	HIA	CP	BBB	CI	AM	AOT	BD
DS2	ZINC31166967	+	−	+	−	−	3.738	0.75
DS1	ZINC54661486	+	+	+	−	−	2.618	0.85
DS2	ZINC13367860	+	+	+	−	−	2.926	0.775
DS1	ZINC78877086	+	−	+	−	−	2.71	0.9
DS2	ZINC31162553	+	−	+	−	−	2.732	0.825
Methiothepin (MT)		+	+	+	+	+	2.045	0.875
Zotepine		+	+	+	+	−	2.824	0.925

HIA human intestinal absorption, *CP* caco-2 permeability, *BBB* blood–brain barrier, *CI* cytochrome P450 2D6 inhibitor, *AM* Ames mutagenesis, *AOT* acute oral toxicity (LD_{50} (kg/mol)), *BD* biodegradation

nervous system (CNS) side effects (Crivori et al. 2000). The results showed that all the selected compounds can cross the BBB with probability ranging from 0.82 to 0.98. The human CYPs catalyze metabolism of many drugs and inhibition leads to the inhibitory or inductive failure of drug metabolism. The computational models in admetSAR are capable of predicting five major CYP isomers (1A2, 2C9, 2C19, 2D6, and 3A4) inhibitors with high accuracy (Cheng et al. 2011). It is evident from the study that none of the selected compounds were found to be potential CYP 2D6 inhibitor. Prediction of the toxicological profiles has been a significant stage in the process of drug design and discovery. Chemical toxicity leads to mutagenicity, carcinogenicity, and other lethal biological effects. The mutagenic potential of a compound is measured in terms of the bacterial reverse mutation assay, Ames test. The admetSAR server predicts chemical mutagenicity from a diverse compound database comprising 4866 mutagens and 3482 nonmutagens using machine learning methods. The predictive accuracy of Ames mutagenicity by the server is 0.843 (Guan et al. 2019). The study suggested that none of the compounds were found to be mutagenic or carcinogenic. The median lethal dose (LD_{50}) is the statistically derived dose required to kill 50% of the test population (Walum 1998). The lower the LD_{50} value of a compound, the compound is more lethal. In this study, the predicted LD_{50} values of all the compounds were observed to be relatively higher (ranging from 2.618 to 3.738 kg/mol) compared to the reference molecules. Among them, ZINC31166967 exhibited the highest LD_{50} value (3.738 kg/mol). The study revealed that these compounds were predicted as non-lethal. Based on the docking results and pharmacokinetic assessments, ZINC31166967, ZINC78877086, and ZINC31162553 were selected for MD simulation to analyze their molecular stability when complexed with 5-HT_{1B}R.

MD simulation studies

MD simulation was carried out to study the dynamic behavior of unligated-5-HT_{1B}R and 5-HT_{1B}–ligand complexes over a given period of time. The trajectories were analyzed for the overall structural stability, residual fluctuations, compactness, and expansion of protein upon interaction with the selected compounds.

RMSD and RMSF analysis

To determine the conformational changes, the RMSD of C_α-atoms of all the systems were calculated. All the systems were stabilized after initial perturbation and showed almost steady-state dynamics (Fig. 6a). The unligated-5-HT_{1B}R

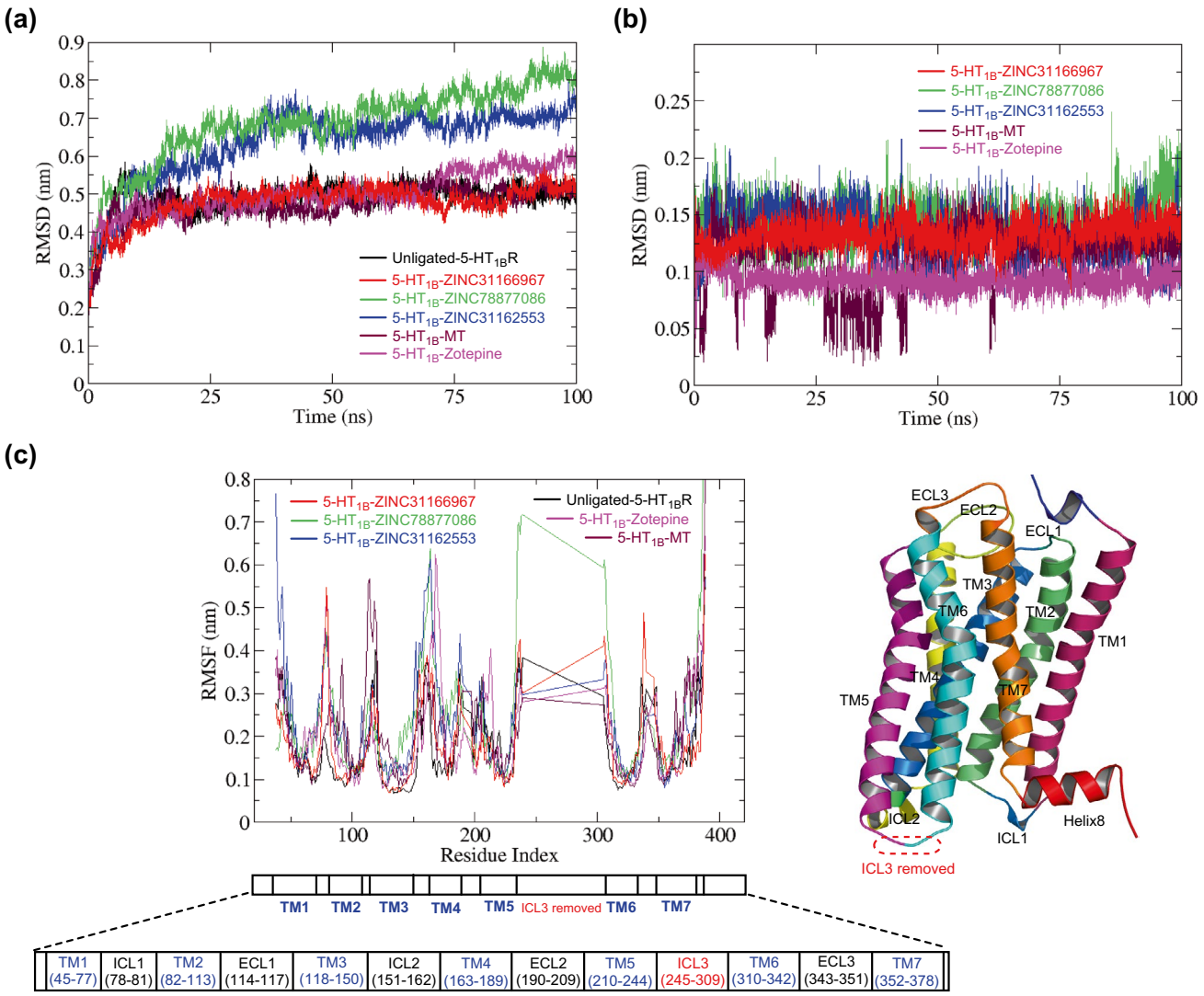

Fig. 6 RMSD and RMSF plots of the unligated, selected compounds and reference docked complex during production MD simulation **a** RMSD values of C_α-atoms **b** Ligand RMSD plots **c** Combined C_α–RMSF plot. *TM* transmembrane, *ICL* intracellular loop, *ECL* extracellular loop

system was equilibrated after ~ 15 ns with an average RMSD value of 0.488 nm. The average value of RMSD for 5-HT_{1B}–MT and 5-HT_{1B}–zotepine were 0.478 and 0.5 nm, respectively. RMSD of 5-HT_{1B}–MT showed equilibration was attained at ~ 10 ns and remained stable at ~ 0.45 nm till the end of the simulation. In case of 5-HT_{1B}–zotepine, the RMSD value was slightly increased to ~ 0.58 nm at around 75 ns and continued till the end. The average RMSD value of 5-HT_{1B}–ZINC31166967, 5-HT_{1B}–ZINC78877086, and 5-HT_{1B}–ZINC31162553 were estimated to be 0.442, 0.686, and 0.625 nm, respectively (Table 5). The RMSD plot of the 5-HT_{1B}–ZINC31166967 showed that the system attained equilibrium at ~ 25 ns and remained stable with marginal fluctuations between 65 and 82 ns. The study suggested that 5-HT_{1B}–ZINC31162553 and 5-HT_{1B}–ZINC78877086 complex displayed comparatively higher RMSD value. The

Table 5 Average values of the RMSD, RMSF and Rg for the simulated systems

System	RMSD (nm)	RMSF (nm)	Rg (nm)
Unligated-5-HT_{1B}R	0.488 ± 0.0407	0.172 ± 0.0889	1.947 ± 0.0125
5-HT_{1B}–ZINC31166967	0.442 ± 0.0402	0.179 ± 0.0950	1.935 ± 0.0155
5-HT_{1B}–ZINC78877086	0.686 ± 0.0894	0.244 ± 0.1499	1.982 ± 0.0204
5-HT_{1B}–ZINC31162553	0.625 ± 0.0631	0.232 ± 0.1168	1.947 ± 0.0270
5-HT_{1B}–MT	0.478 ± 0.0475	0.203 ± 0.1011	1.975 ± 0.0170
5-HT_{1B}–Zotepine	0.500 ± 0.0562	0.201 ± 0.1095	1.936 ± 0.1192

5-HT_{1B}–ZINC31162553 complex exhibited steady RMSD value of ~ 0.67 nm after 45 ns. The RMSD value gradually increased in 5-HT_{1B}–ZINC78877086 and reached ~ 0.7 nm at ~ 25 ns and continued up to ~ 50 ns. The value increased further and persisted at ~ 0.78 nm. The study revealed that the 5-HT_{1B}–ZINC31166967 complex was highly stable compared to others throughout the entire simulation. The RMSD of all the ligands was less than protein RMSD and found to be between 0.1 and 0.2 nm except for MT, which showed fluctuation up to ~ 60 ns and converged to a constant value of ~ 0.13 nm (Fig. 6b). The less ligand RMSD indicates that the ligand was stable within the binding pocket of the protein. The RMSD results suggested that ZINC31166967 among all the selected compounds formed a stable complex with 5-HT_{1B}R and retained overall stability throughout 100 ns of simulation.

The local residue flexibility was evaluated by calculating the RMSF of C_{α}-atoms of all the systems. The helices and sheets show less flexibility, while loops and turns show higher flexibility (Shukla et al. 2020). The RMSF profiles pointed out the regions of fluctuations in 5-HT_{1B}R (Fig. 6c). The average RMSF value was found to be 0.172 nm for unligated-5-HT_{1B}R, 0.203 nm for 5-HT_{1B}–MT, and 0.201 nm for 5-HT_{1B}–Zotepine, respectively. Similarly, 5-HT_{1B}–ZINC31166967, 5-HT_{1B}–ZINC78877086, and 5-HT_{1B}–ZINC31162553 system showed RMSF values of 0.179, 0.244, and 0.232 nm, respectively. ZINC78877086 caused more fluctuation upon binding with 5-HT_{1B}R as compared to others. The average RMSF value of unligated-5-HT_{1B}R and 5-HT_{1B}–ZINC31166967 were estimated to be identical. The study revealed that most of the fluctuations were observed in the loop regions (ECL1–ECL3 and ICL1–ICL3) of the protein in all systems (Fig. 6c). The RMSF value of the orthosteric binding pocket residues remained less than ~ 0.2 nm (Supplementary data Fig. S1). The study suggested that the binding of ZINC31166967 to 5-HT_{1B}R showed less residue flexibility and hence more stable compared to 5-HT_{1B}–ZINC78877086 and 5-HT_{1B}–ZINC31162553 complex.

Rg, SASA and hydrogen bond analysis

The structural compactness of the protein–ligand complex was determined by calculating the backbone Rg. The average Rg value for unligated-5-HT_{1B}R, 5-HT_{1B}–MT, and 5-HT_{1B}–Zotepine were 1.947, 1.975, and 1.936 nm, respectively (Table 5). The 5-HT_{1B}–ZINC31166967 and 5-HT_{1B}–ZINC31162553 showed an average Rg value of 1.935 and 1.947 nm, respectively (Fig. 7a), which was found to be similar to the unligated-5-HT_{1B}R system. However, 5-HT_{1B}–ZINC78877086 exhibited relatively higher Rg value at ~ 44–72 ns and stabilized towards the end of the simulation with an average Rg value of 1.982 nm. The unligated-5-HT_{1B}R and complexes showed almost similar Rg value, which suggested that the overall structure and the compactness of the protein was not much affected by ligand binding. It is evident from the study that ZINC31166967 and ZINC31162553 formed comparatively more stable and compact structure with 5-HT_{1B}R.

The solvent environment has an essential role in maintaining the protein folding-unfolding dynamics and protein–ligand interactions. SASA was calculated to assess the structural stability of the complexes under solvent conditions. SASA values for unligated-5-HT_{1B}R, 5-HT_{1B}–MT, and 5-HT_{1B}–Zotepine were found to be 148.45, 152.13, and 153.16 nm^2 respectively, whereas the complex structure of 5-HT_{1B}–ZINC31166967, 5-HT_{1B}–ZINC78877086, and 5-HT_{1B}–ZINC31162553 revealed average SASA values of 160.08, 154.12, and 159.02 nm^2, respectively (Fig. 7b). The binding of the selected compounds showed marginal expansion in the 5-HT_{1B}R conformation that allows more accessibility and interaction with the solvents.

The specificity, adsorption, and metabolism of a drug depend on the hydrogen bonds formed between the drug and target protein. Total number of hydrogen bonds was calculated from the MD trajectories to determine the binding affinity of selected compounds and receptor protein. Both MT and zotepine docked complexes displayed two hydrogen bonds, whereas the ZINC31166967, ZINC78877086, and ZINC31162553 docked complexes showed the number of hydrogen bonds between 0–8, 0–3, and 0–12, respectively (Fig. 7c). The maximum number of hydrogen bonds was observed in 5-HT_{1B}–ZINC31162553 followed by the 5-HT_{1B}–ZINC31166967 complex. The number of hydrogen bonds remained steady throughout the simulation for all the three docked complexes. The molecular docking, SASA, and hydrogen bonding interaction studies indicated that ZINC31166967 and ZINC31162553 fitted well within the binding pocket and formed stable conformation through hydrogen bonds and hydrophobic interactions. It is evident from the study that the compounds ZINC31166967 and ZINC31162553 exhibited relatively higher stable interactions between the receptor and ligand complexes compared to reference molecules such as MT and zotepine, which indicated that the maximum region of 5-HT_{1B}R accessible to the solvent molecules supplementing higher hydrogen bonds. In the case of ZINC31166967 and ZINC31162553, ligand occupancy in the binding pocket is more because of the bulkier group as compared to MT and zotepine (Supplementary data Fig. S2).

Conclusion

The structural analogs of MT and natural compounds were computationally screened against the binding pockets of 5-HT_{1B}R to identify the receptor-specific ligands.

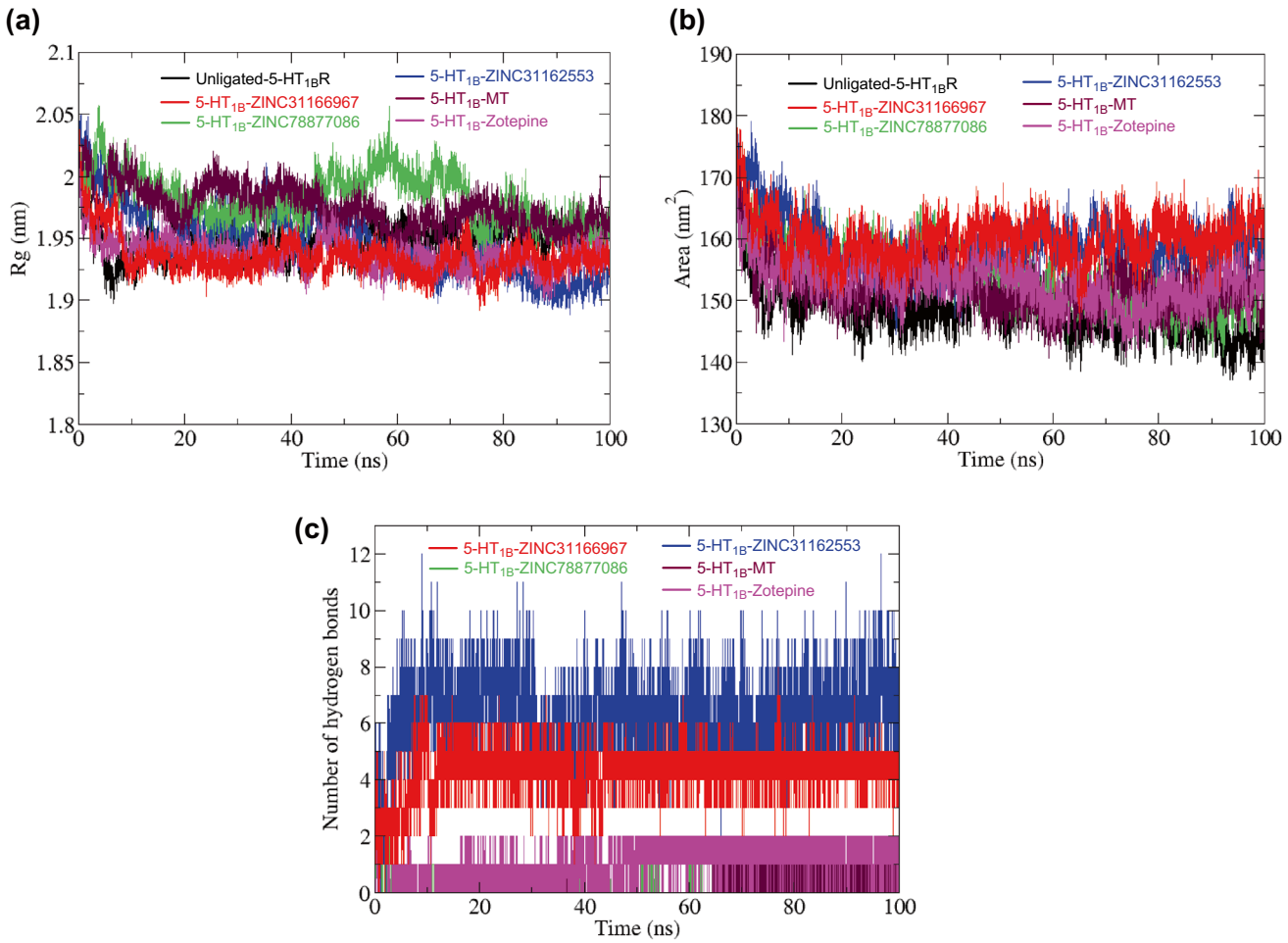

Fig. 7 Radius of gyration (Rg), solvent accessible surface area (SASA) and hydrogen bonds during the production MD simulation **a** Rg plot of backbone atoms of unligated-5-HT_{1B}R and ligand docked complexes **b** SASA plot of 5-HT_{1B}-docked complexes **c** Total number of hydrogen bonds between ligands and 5-HT_{1B}R

Compounds with higher binding affinities than MT (− 8.8 kcal/mol) were further docked with other 5-HTRs (5-HT_{2A}R, 5-HT_{2B}R, and 5-HT_{2C}R) and compounds with lower binding affinities towards these receptors were selected. Out of all the screened compounds, five compounds were found to be selective for 5-HT_{1B}R over other 5-HTRs. The binding energies of the selected compounds with 5-HT_{1B}R varied between − 10.1 and − 9.1 kcal/mol. The ZINC31166967 showed the lowest binding energy of − 10.1 kcal/mol among selected compounds. Based on molecular docking and ADMET assessments, three compounds (ZINC31166967, ZINC78877086, and ZINC31162553) complexed with 5-HT_{1B}R were considered for MD simulation to understand their structural stability. The MD simulation analysis showed that ZINC31166967 and ZINC31162553 displayed reasonable structural stability within the binding pocket of 5-HT_{1B}R as evidenced from RMSD, RMSF, SASA, and hydrogen bonding data. Thus, the molecular docking, pharmacokinetics assessments, and MD simulation studies identified ZINC31166967 and ZINC31162553 as 5-HT_{1B}R selective ligands. However, a comprehensive computational and experimental investigation is required to establish the selectivity of these compounds, because 14 subtypes (including 5-HT_3R) exist in the 5-HTR family. Further, the study could be used to design new derivatives to develop more specific and effective inhibitors for 5-HT_{1B}R.

Supplementary Information The online version contains supplementary material available at https://doi.org/10.1007/s42485-021-00069-8.

Acknowledgements The authors would like to thank the Supercomputing Facility for Bioinformatics and Computational Biology (SCFBio), IIT Delhi and Department of Biotechnology and Bioinformatics, Sambalpur University for providing computational facilities.

Funding None.

Availability of data and materials Not applicable.

Code availability Not applicable.

Declarations

Conflict of interest The authors declare no conflict of interest.

Ethical approval This review does not contain any studies with human participants or animals performed by the author.

Consent to participate Not applicable.

Consent for publication Manuscript has been read and approved by all named authors.

References

Abraham MJ, Murtola T, Schulz R, Páll S, Smith JC, Hess B, Lindahl E (2015) GROMACS: high performance molecular simulations through multi-level parallelism from laptops to supercomputers. SoftwareX 1:19–25. https://doi.org/10.1016/j.softx.2015.06.001

Ballesteros JA, Weinstein H (1995) Integrated methods for the construction of three-dimensional models and computational probing of structure-function relations in G protein-coupled receptors. Methods Neurosci 25:366–428. https://doi.org/10.1016/S1043-9471(05)80049-7

Berger M, Gray JA, Roth BL (2009) The expanded biology of serotonin. Annu Rev Med 60:355–366. https://doi.org/10.1146/annurev.med.60.042307.110802

Berman HM, Westbrook J, Feng Z, Gilliland G, Bhat TN, Weissig H, Shindyalov IN, Bourne PE (2000) The protein data bank. Nucleic Acids Res 28:235–242. https://doi.org/10.1093/nar/28.1.235

Bhowmik D, Sharma RD, Prakash A, Kumar D (2021) Identification of Nafamostat and VR23 as COVID-19 drug candidates by targeting 3CLpro and PLpro. J Mol Struct 1233:130094. https://doi.org/10.1016/j.molstruc.2021.130094

Bussi G, Donadio D, Parrinello M (2007) Canonical sampling through velocity rescaling. J Chem Phys 126:014101. https://doi.org/10.1063/1.2408420

Cao J, LaRocque E, Li D (2013) Associations of the 5-hydroxytryptamine (serotonin) Receptor 1B gene (HTR1B) with alcohol, cocaine, and heroin abuse. Am J Med Genet B 162:169–176. https://doi.org/10.1002/ajmg.b.32128

Cheng F, Yu Y, Shen J, Yang L, Li W, Liu G, Lee PW, Tang Y (2011) Classification of cytochrome P450 inhibitors and noninhibitors using combined classifiers. J Chem Inf Model 51:996–1011. https://doi.org/10.1021/ci200028n

Crivori P, Cruciani G, Carrupt P-A, Testa B (2000) Predicting blood–brain barrier permeation from three-dimensional molecular structure. J Med Chem 43:2204–2216. https://doi.org/10.1021/jm990968+

Dallakyan S, Olson AJ (2015) Small-molecule library screening by docking with PyRx. In: Hempel J, Williams C, Hong C (eds) Chemical biology in: chemical biology, methods in molecular biology. Humana Press, New York. https://doi.org/10.1007/978-1-4939-2269-7_19

Deserno M, Holm C (1998) How to mesh up Ewald sums. II. An accurate error estimate for the particle–particle–particle-mesh algorithm. J Chem Phys 109:7694–7701. https://doi.org/10.1063/1.477415

Essmann U, Perera L, Berkowitz ML, Darden T, Lee H, Pedersen LG (1995) A smooth particle mesh Ewald method. J Chem Phys 103:8577–8593. https://doi.org/10.1063/1.470117

Fernandes J, Gattass CR (2009) Topological polar surface area defines substrate transport by multidrug resistance associated protein 1 (MRP1/ABCC1). J Med Chem 52:1214–1218. https://doi.org/10.1021/jm801389m

Fredriksson R, Lagerström MC, Lundin L-G, Schiöth HB (2003) The G-protein-coupled receptors in the human genome form five main families. Phylogenetic analysis, paralogon groups, and fingerprints. Mol Pharmacol 63:1256–1272. https://doi.org/10.1124/mol.63.6.1256

Guan L, Yang H, Cai Y, Sun L, Di P, Li W, Liu G, Tang Y (2019) ADMET-score—a comprehensive scoring function for evaluation of chemical drug-likeness. Med Chem Commun 10:148–157. https://doi.org/10.1039/C8MD00472B

Hauser AS, Chavali S, Masuho I, Jahn LJ, Martemyanov KA, Gloriam DE, Babu MM (2018) Pharmacogenomics of GPCR drug targets. Cell 172:41–54. https://doi.org/10.1016/j.cell.2017.11.033

Hess B, Bekker H, Berendsen HJ, Fraaije JG (1997) LINCS: a linear constraint solver for molecular simulations. J Comput Chem 18:1463–1472. https://doi.org/10.1002/(SICI)1096-987X(199709)18:12%3c1463::AID-JCC4%3e3.0.CO;2-H

Hou T, Zhang W, Xia K, Qiao X, Xu X (2004) ADME evaluation in drug discovery. 5. Correlation of Caco-2 permeation with simple molecular properties. J Chem Inf Comput Sci 44:1585–1600. https://doi.org/10.1021/ci049884m

Hummer G (1995) The numerical accuracy of truncated Ewald sums for periodic systems with long-range Coulomb interactions. Chem Phys Lett 235:297–302. https://doi.org/10.1016/0009-2614(95)00117-M

Irwin JJ, Sterling T, Mysinger MM, Bolstad ES, Coleman RG (2012) ZINC: a free tool to discover chemistry for biology. J Chem Inf Model 52:1757–1768. https://doi.org/10.1021/ci3001277

Jaillet L, Artemova S, Redon S (2017) IM-UFF: extending the universal force field for interactive molecular modeling. J Mol Graph Model 77:350–362. https://doi.org/10.1016/j.jmgm.2017.08.023

Kim K, Che T, Panova O, DiBerto JF, Lyu J, Krumm BE, Wacker D, Robertson MJ, Seven AB, Nichols DE (2020) Structure of a hallucinogen-activated Gq-coupled 5-HT2A serotonin receptor. Cell 182:1574–1588. https://doi.org/10.1016/j.cell.2020.08.024

Kimura KT, Asada H, Inoue A, Kadji FMN, Im D, Mori C, Arakawa T, Hirata K, Nomura Y, Nomura N (2019) Structures of the 5-HT 2A receptor in complex with the antipsychotics risperidone and zotepine. Nat Struct Mol Biol 26:121–128. https://doi.org/10.1038/s41594-018-0180-z

Lanfumey L, Hamon M (2004) 5-HT1 receptors. Curr Drug Targets CNS Neurol Disord 3:1–10. https://doi.org/10.2174/1568007043482570

Laskowski RA, Swindells MB (2011) LigPlot+: multiple ligand–protein interaction diagrams for drug discovery. J Chem Inf Model 51:2778–2786. https://doi.org/10.1021/ci200227u

Lipinski CA (2004) Lead-and drug-like compounds: the rule-of-five revolution. Drug Discov Today Technol 1:337–341. https://doi.org/10.1016/j.ddtec.2004.11.007

Lipinski CA (2008) Compound properties and drug quality. The practice of medicinal chemistry, Elsevier, pp 481–490. https://doi.org/10.1016/B978-0-12-374194-3.00022-6

McCorvy JD, Roth BL (2015) Structure and function of serotonin G protein-coupled receptors. Pharmacol Ther 150:129–142. https://doi.org/10.1016/j.pharmthera.2015.01.009

McCorvy JD, Wacker D, Wang S, Agegnehu B, Liu J, Lansu K, Tribo AR, Olsen RH, Che T, Jin J (2018) Structural determinants of 5-HT 2B receptor activation and biased agonism. Nat Struct Mol Biol 25:787–796. https://doi.org/10.1038/s41594-018-0116-7

Oostenbrink C, Villa A, Mark AE, Van Gunsteren WF (2004) A biomolecular force field based on the free enthalpy of hydration and solvation: the GROMOS force-field parameter sets 53A5 and 53A6. J Comput Chem 25:1656–1676. https://doi.org/10.1002/jcc.20090

Oostenbrink C, Soares TA, Van der Vegt NF, Van Gunsteren WF (2005) Validation of the 53A6 GROMOS force field. Eur Biophys J 34:273–284. https://doi.org/10.1007/s00249-004-0448-6

Parrinello M, Rahman A (1981) Polymorphic transitions in single crystals: a new molecular dynamics method. J Appl Phys 52:7182–7190. https://doi.org/10.1063/1.328693

Peng Y, McCorvy JD, Harpsøe K, Lansu K, Yuan S, Popov P, Qu L, Pu M, Che T, Nikolajsen LF (2018) 5-HT2C receptor structures reveal the structural basis of GPCR polypharmacology. Cell 172:719–730. https://doi.org/10.1016/j.cell.2018.01.001

Pettersen EF, Goddard TD, Huang CC, Couch GS, Greenblatt DM, Meng EC, Ferrin TE (2004) UCSF Chimera–a visualization system for exploratory research and analysis. J Comput Chem 25:1605–1612. https://doi.org/10.1002/jcc.20084

Pham The H, González-Álvarez I, Bermejo M, Mangas Sanjuan V, Centelles I, Garrigues TM, Cabrera-Pérez MÁ (2011) In silico prediction of Caco-2 cell permeability by a classification QSAR approach. Mol Inform 30:376–385. https://doi.org/10.1002/minf.201000118

Rappé AK, Casewit CJ, Colwell K, Goddard WA III, Skiff WM (1992) UFF, a full periodic table force field for molecular mechanics and molecular dynamics simulations. J Am Chem Soc 114:10024–10035. https://doi.org/10.1021/ja00051a040

Sander T, Freyss J, von Korff M, Rufener C (2015) DataWarrior: an open-source program for chemistry aware data visualization and analysis. J Chem Inf Model 55:460–473. https://doi.org/10.1021/ci500588j

Sari Y (2004) Serotonin1B receptors: from protein to physiological function and behavior. Neurosci Biobehav Rev 28:565–582. https://doi.org/10.1016/j.neubiorev.2004.08.008

Schüttelkopf AW, Van Aalten DM (2004) PRODRG: a tool for high-throughput crystallography of protein–ligand complexes. Acta Crystallogr D 60:1355–1363. https://doi.org/10.1107/S0907444904011679

Shukla R, Shukla H, Kalita P, Tripathi T (2018) Structural insights into natural compounds as inhibitors of *Fasciola gigantica* thioredoxin glutathione reductase. J Cell Biochem 119:3067–3080. https://doi.org/10.1002/jcb.26444

Shukla R, Shukla H, Tripathi T (2019) Structural and energetic understanding of novel natural inhibitors of *Mycobacterium tuberculosis* malate synthase. J Cell Biochem 120:2469–2482. https://doi.org/10.1002/jcb.27538

Shukla R, Shukla H, Tripathi T (2020) Structure-based discovery of phenyl-diketo acids derivatives as *Mycobacterium tuberculosis* malate synthase inhibitors. J Biomol Struct Dyn 39:2945–2958. https://doi.org/10.1080/07391102.2020.1758787

Slassi A (2002) Recent advances in 5-HT1B/1D receptor antagonists and agonists and their potential therapeutic applications. Curr Top Med Chem 2:559–574. https://doi.org/10.2174/1568026023393903

Sterling T, Irwin JJ (2015) ZINC 15–ligand discovery for everyone. J Chem Inf Model 55:2324–2337. https://doi.org/10.1021/acs.jcim.5b00559

Tiger M, Varnäs K, Okubo Y, Lundberg J (2018) The 5-HT 1B receptor-a potential target for antidepressant treatment. Psychopharmacol 235:1317–1334. https://doi.org/10.1007/s00213-018-4872-1

Trott O, Olson AJ (2010) AutoDock Vina: improving the speed and accuracy of docking with a new scoring function, efficient optimization, and multithreading. J Comput Chem 31:455–461. https://doi.org/10.1002/jcc.21334

Wacker D, Wang C, Katritch V, Han GW, Huang XP, Vardy E, McCorvy JD, Jiang Y, Chu M, Siu FY, Liu W (2013) Structural features for functional selectivity at serotonin receptors. Science 340:615–619. https://doi.org/10.1126/science.1232808

Wacker D, Wang S, McCorvy JD, Betz RM, Venkatakrishnan A, Levit A, Lansu K, Schools ZL, Che T, Nichols DE (2017) Crystal structure of an LSD-bound human serotonin receptor. Cell 168:377–389. https://doi.org/10.1016/j.cell.2016.12.033

Walum E (1998) Acute Oral Toxicity. Environ Health Persp 106:497–503. https://doi.org/10.1289/ehp.98106497

Wang C, Jiang Y, Ma J, Wu H, Wacker D, Katritch V, Han GW, Liu W, Huang X-P, Vardy E (2013) Structural basis for molecular recognition at serotonin receptors. Science 340:610–614. https://doi.org/10.1126/science.1232807

Webb B, Sali A (2016) Comparative protein structure modeling using MODELLER. Curr Protoc Bioinform 54:5.6.1-5.6.37. https://doi.org/10.1002/cpbi.3

Yang H, Lou C, Sun L, Li J, Cai Y, Wang Z, Li W, Liu G, Tang Y (2019) admetSAR 2.0: web-service for prediction and optimization of chemical ADMET properties. Bioinformatics 35:1067–1069. https://doi.org/10.1093/bioinformatics/bty707

Yin W, Zhou XE, Yang D, de Waal PW, Wang M, Dai A, Cai X, Huang CY, Liu P, Wang X, Yin Y (2018) Crystal structure of the human 5-HT 1B serotonin receptor bound to an inverse agonist. Cell Discov 4:12. https://doi.org/10.1038/s41421-018-0009-2

Zhang T, Li Y, Gao P, Shao Q, Shao M, Zhang M, Zhang J, Duan X, Liu Z, Gan L (2019) SW_GROMACS: accelerate GROMACS on Sunway TaihuLight. Proceedings of the International Conference for High Performance Computing, Networking, Storage and Analysis, pp 1–14. https://doi.org/10.1145/3295500.3356190

Zhao YH, Abraham MH, Le J, Hersey A, Luscombe CN, Beck G, Sherborne B, Cooper I (2002) Rate-limited steps of human oral absorption and QSAR studies. Pharm Res 19:1446–1457. https://doi.org/10.1023/A:1020444330011